

Modeling of fatigue wear of a layered elastic foundation in contact with periodic system of dies

I.G. Goryacheva¹, E.V. Torskaya¹

¹ *Institute for Problems in Mechanics RAS, Moscow, Russia*

1. Introduction

Coatings are widely applied in friction conjunctions to increase the lifetime of the details. Coating fracture may occur in different ways. The surface wear is typical for the case of soft coatings; for the case of relatively hard coatings the wear process may be accompanied by the failure of the coating–substrate bond and the coating delaminating [1].

Therefore, it is important to model the contact-wear fracture of the coating under its cyclic friction loading. The general approach to the investigation of the contact-wear fracture of rough bodies is presented in [2, 3]. The model of fatigue fracture of a homogeneous elastic half-space in sliding contact with a periodic system of indenters under different types of loading is developed in [4]. The model permits one to describe two phenomena - the simultaneous process of continuous surface wear, and the separation of a layer of finite thickness - by the same mechanisms of damage accumulation.

To model the contact wear fracture of elastic bodies, it is necessary to know the distribution of stresses in the loaded body. For coated elastic bodies the model of two-layered elastic foundation is usually used to determine the contact characteristics (the size of contact zone and contact pressure distribution) and stresses inside the layer and the substrate. A contact problem for a punch and a two-layered elastic foundation can be solved using the integral transforms, i.e. method such as Fourier transform for 2-D problem and Hankel transform for frictionless axisymmetric problem [5-8]. Such method is mostly analytical and usually assumes some calculations at the final step because of the complication form of inverse integral transforms. The computation simplicity and the high accuracy of results make this method suitable for axisymmetric and 2-D problems. The numerical methods are preferable for more complicated 3-D contact problems. The influence of the surface microgeometry parameters on the contact pressure and internal stresses inside the elastic layer bonded to the elastic substrate is analysed in [9–11]. The system of dies modelled a rough surface in contact interaction. The contact of real rough surfaces with coated bodies is considered numerically in [12-14]. The influence of friction on the distribution of internal stresses in the layered elastic half-space is studied in [8].

A model to study the kinetics of fatigue fracture of a layered elastic half-space in contact with a periodic system of indenters, which models the surface micro roughness, is presented here.

2. Problem formulation and the method of solution.

The sliding of a periodic system of spherical indenters of radius R on the boundary of a layered elastic half-space (Fig. 1) is considered. The indenters are located at the nodes of a hexagonal lattice with period l , and the direction of motion coincides with the direction of the axis (Ox). The system is loaded by the period-averaged nominal pressure p_n and the tangential stresses τ_n , which are determined by the Coulomb–Amonton law, i.e., $\tau_n = \mu p_n$, where μ is the coefficient of the sliding friction. The layered elastic half-space consists of an elastic layer of thickness h and an elastic half-space; elastic properties of the layer and the half-space are characterized by the elasticity moduli E_i and the Poisson ratios ν_i ($i = 1, 2$ for the layer and for the half-space, respectively).

During sliding the cyclic loads generate an inhomogeneous cyclic field of internal stresses, which is the cause of accumulation of fatigue damage and the fracture of the material surface layers. The model of the damage accumulation process proposed includes the following steps in calculations:

- Calculation of the contact pressure for the periodic contact problem.
- Calculation of the internal stresses taking into account the friction forces for the multiple contact.
- Calculation of the damage accumulation function based on the appropriate phenomenological approach for description of the damage accumulation process.
- Analysis of the fracture kinetics.

2.1. The contact problem solution.

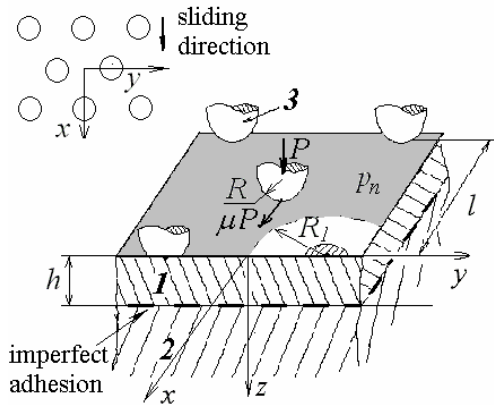


Fig.1 Scheme of the periodic friction contact

For a system of axially symmetrical indenters located at the nodes of a hexagonal lattices (Fig. 1), the relation between the load P acting on each indenter and the nominal pressure p_n is the following

$$P = (\sqrt{3}/2) p_n l^2 \quad (2.1)$$

where l is the lattice period.

The conditions at the interface ($z = h$) between layer and substrate are determined by the relations

$$\begin{aligned} \sigma_z^{(1)} &= \sigma_z^{(2)}, \quad \tau_{xz}^{(1)} = \tau_{xz}^{(2)}, \quad \tau_{yz}^{(1)} = \tau_{yz}^{(2)}, \quad w^{(1)} = w^{(2)} \\ \tau_{xz}^{(1)} &= \frac{1}{k} (v_x^{(1)} - v_x^{(2)}), \quad \tau_{yz}^{(1)} = \frac{1}{k} (v_y^{(1)} - v_y^{(2)}) \end{aligned} \quad (2.2)$$

Here $\sigma_z^{(i)}, \tau_{xz}^{(i)}, \tau_{yz}^{(i)}$ are the stresses, and $w^{(i)}, v_x^{(i)}, v_y^{(i)}$ are normal and tangential displacements of the elastic layer ($i = 1$) and the elastic substrate ($i = 2$). Coefficient k is the parameter of imperfect adhesion between the layer and the substrate; if $k=0$ the perfect adhesion takes place.

Under the assumption that the influence of shear stresses on the distribution of contact normal stress is negligibly small, the following boundary conditions on the upper layer surface ($z = 0$) written in polar coordinates (r, θ) are considered:

$$\begin{aligned} w(r) &= f(r) + \delta, & 0 \leq r \leq a \\ \sigma_z^{(1)} &= 0, & a < r < R_1 \\ \sigma_z^{(1)} &= -p_n, & R_1 \leq r < \infty \\ \tau_{rz}^{(1)} &= \tau_{\theta z}^{(1)} = 0, & 0 \leq r < \infty \end{aligned} \quad (2.3)$$

Here $f(r)$ is the indenter shape, δ is the indenter displacement along the axis (Oz), a is the radius of a contact zone ω_i .

The boundary conditions (2.3) are obtained using the localization principle formulated and proved in [2] for the case of penetration of a periodic system of indenters into the elastic half-space. The accuracy of the solution based on the problem formulation with boundary conditions (2.3) in comparison with one obtained from the exact problem formulation for the periodic system of indenters on the elastic half-space is also estimated there. To obtain the pressure distribution for a chosen indenter inside a contact zone $r \leq a$, the action of the other indenters is replaced by the action of the nominal pressure p_n distributed outside the circle with radius R_1 (Fig. 1). The radius R_1 is determined from the equilibrium equation and (2.1) as

$$R_1 = (P / (p_n))^{1/2} = (\sqrt{3} / (2\pi))^{1/2} l \cong 0.525 l \quad (2.4)$$

The equilibrium equation has the form

$$P = \int_0^a \int_0^{2\pi} p_s(r) r dr d\varphi \quad (2.5)$$

where $r = \sqrt{(x - x_c)^2 + (y - y_c)^2}$ (x_c and y_c are the coordinates of the center of the considered indenter), $p_s(r)$ is the contact pressure distributed in each contact spot ω_i ($p_s(r) = -\sigma_z(r)$, $r \in \omega_i$).

The solution of the axisymmetrical contact problem for the layered elastic half-space with boundary conditions (2.2) and (2.3) is obtained by the method presented in [9]. It consists of two stages. The first stage is to find the shape $g(r)$ of the deformed surface of the unloaded circular zone $0 \leq r \leq R_1$ caused by the pressure p_n applied outside it ($R_1 \leq r < +\infty$); the following boundary conditions at the upper layer surface ($z=0$) are considered

$$\begin{aligned} \sigma_z^{(1)} &= 0, & 0 < r < R_1 \\ \sigma_z^{(1)} &= -p_n, & R_1 \leq r < \infty \\ \tau_{rz}^{(1)} &= \tau_{\theta z}^{(1)} = 0, & 0 \leq r < \infty \end{aligned} \quad (2.6)$$

The problem is solved by using the Hankel integral transforms [9, 11].

At the second stage, the function $g(r)$ is used to formulate the boundary conditions at the upper surface ($z=0$) of the elastic layer. To solve the contact problem, we divide the contact zone into K rings of equal thickness and determine the contact pressure as a piecewise function. Using the relations between the load and displacements [9] we find the influence coefficients k_j^i , and reduce the problem to the following system of equations to determine the contact pressure:

$$\begin{aligned} p_1 k_1^{(i)} + p_2 k_2^{(i)} + \dots + p_k k_k^{(i)} &= f'(r_i) \\ i &= 1, 2, \dots, K-1 \end{aligned} \quad (2.7)$$

$$\begin{aligned} \pi \sum_{i=1}^K p_i (r_i^2 - r_{i-1}^2) &= P \\ f'(r) &= (f(r) - f(a)) - (g(r) - g(a)) \end{aligned}$$

To find the unknown radius of the contact zone, the condition of zero pressure on the boundary of the contact zone is used and the iteration method is applied.

The analysis of the influence of the indenter shape, the surface layer relative thickness, and its mechanical characteristics on the distribution of contact pressures is presented in [11].

2.2 Calculation of the internal stresses

The internal stresses in the layered elastic half-space are determined from the following conditions on the upper layer surface ($z = 0$):

$$\begin{aligned} \sigma_z^{(1)}(x, y) &= p_s(x, y), \quad \tau_{xz}^{(1)} = -\mu p_s(x, y), \quad (x, y) \in \omega_i \\ \sigma_z^{(1)} &= 0, \quad \tau_{xz}^{(1)} = 0, \quad (x, y) \notin \omega_i \\ \tau_{yz}^{(1)} &= 0, \quad -\infty < x, y < \infty \end{aligned} \quad (2.8)$$

At the interface ($z = h$) the boundary conditions are given by (2.2).

The problem is solved by using the boundary element method. The contact zone is considered as a system of squares with side Δs with a constant tangential stresses inside each square. The boundary conditions (2.9) are transformed to

$$\begin{aligned} \tau_{xz}^{(1)} &= -\mu \gamma_j^k p_0, \quad -a + \frac{a}{\Delta s}(j-1) < x < -a + \frac{a}{\Delta s} j, \quad -a + \frac{a}{\Delta s}(k-1) < y < -a + \frac{a}{\Delta s} k \\ \sigma_z^{(1)} &= \gamma_j^k p_0, \quad \tau_{xz}^{(1)} = 0, \quad \tau_{yz}^{(1)} = 0, \quad -\infty < (x, y) < \infty \end{aligned} \quad (2.9)$$

Here p_0 is the maximum contact pressure, and the dimensionless coefficients γ_j^k ($0 \leq \gamma_j^k \leq 1$), which determine the contact tangential stresses in each square are obtained from the contact problem solution.

The problem is reduced to the determination of the internal stresses due to a constant distributed load. It can be solved by the method based on double integral Fourier transforms [16]. For this case the boundary conditions are the following

$$\overline{\gamma_j^k}(\alpha, \beta) = \int_0^{\infty} \int_0^{\infty} (\mu \gamma_j^k p_0 x) e^{-i(\alpha x + \beta y)} dx dy \quad (2.10)$$

$$-a + \frac{a}{\Delta s}(j-1) < x < -a + \frac{a}{\Delta s}j, \quad -a + \frac{a}{\Delta s}(k-1) < y < -a + \frac{a}{\Delta s}k$$

The method based on the localization principle and the superposition is used to take into account mutual effect.

2.3. Model of the contact fatigue in the surface layer.

To model the contact fatigue in the surface layer, we use a macroscopic approach, developed in [2]-[4]. It involves the construction of the positive function $Q(M, t)$ non-decreasing in time; the function characterizes the material damage at the point $M(x, y, z)$, and depends on the stress amplitude values at this point. To study damage accumulation, the model of the damage linear summation is used (the damage increment at each moment does not depend on the value of the already accumulated damage). The fracture occurs at the time instant t^* at which this function reaches a threshold level at some point.

There are various physical approaches to the damage modeling, in which the rate of damage accumulation $\partial Q(x, y, z, t)/\partial t$ is considered as a function of stress at the given point, the temperature, and other parameters depending on the fracture mechanism, the type of material, and some other factors [3]. For the present study, we assume that the relation between the fatigue accumulation rate $\partial Q(x, y, z, t)/\partial t$ and the amplitude value $\Delta \tau_1$ of the principal shear stress at the point has the following form

$$q(x, y, z, t) = \frac{\partial Q(x, y, z, t)}{\partial t} = c (\Delta \tau_1(x, y, z, t))^m \quad (2.11)$$

where c and m are some experimentally determined constants and $\Delta \tau_1(x, y, z, t)$ is the amplitude value of the principal shear stress at the point (x, y, z) for one period of sliding loading.

The problem is periodic, that's why the damage function is independent of the coordinates x and y and depends only on the coordinate z and the time t (the time can be evaluated by the number of cycles N). The damage $Q(z, N)$, which is accumulated at fixed point z during N cycles, is calculated from the relation

$$Q(z, N) = \int_0^N q_n(z, n) dn + Q_0(z) \quad (2.12)$$

where $Q_0(z)$ is the distribution of the initial damage in the material and $q_n(z, n)$ is the rate of the damage accumulation independent of the coordinates x, y .

The fracture occurs as the damage at some depth z^* reaches the critical value. In a normalized system this condition is

$$Q(z^*, N^*) = 1 \quad (2.13)$$

where N^* is the number of cycles before the fracture initiation.

Calculation of the stress distribution in the elastic layer makes it possible to find the maximum amplitude values of the principal shear stresses along the axis (Ox), which coincides with the sliding direction. The maximum amplitude values occur in the plane passing through the geometric center of the contact zone (x_c, y_c). The function $\Delta\tilde{\tau}_1(z, n)$ characterizes the maximum amplitude values of the principal shear stress.

To calculate the number N^* of cycles before the fracture initiation, the following relation is obtained from (2.11)-(2.13):

$$\int_0^L c(\Delta\tilde{\tau}_1(z, n))^m dn + Q_0(z) = 1 \quad (2.14)$$

The damage function $Q(z, N)$ is calculated by summation. In the assumption of zero initial damage the number of cycles N^* before the first fracture at the depth h_1 is calculated from the following relation:

$$N^* c(\max_z \Delta\tilde{\tau}_1(z))^m = 1, \quad 0 \leq z \leq h \quad (2.15)$$

If the maximum value of the function $\Delta\tilde{\tau}_1(z)$ takes place inside the surface layer at a depth z^* , the delaminating of the layer of thickness z^* occurs, and the rest part of the surface layer comes into contact. The damage at this layer of thickness ($h-z^*$) is determined by the function

$$Q^*(z) = N^* c(\Delta\tilde{\tau}_1(z, 0))^m$$

The damage distribution Q^* must be taken into account in the further study of the process of damage accumulation.

After the material detachment the function $Q^*(z)$ at the newly formed surface has a value close to the critical one. The surface wear occurs, and the elastic layer thickness decrease continuously after the first fracture. The next subsurface maximum may take place, and it may cause the second act of delaminating.

If the function $\Delta\tilde{\tau}_1(z, 0)$ has its maximum at the surface, the continuous surface wear takes place. The damage can also grow up at the interface ($z=h$).

3. Results and discussion.

The algorithm described above is used to calculate the kinetics of the fatigue wear of a layered elastic half-space by a periodic system of indenters of spherical shape located at the nodes of a hexagonal lattice. In the case of small strains, the indenter shape is described by the function $f(r) = r^2/(2R)$, where R is the indenter

radius. It is obtained that contact and internal stresses depend on the following dimensionless parameters: the coating relative hardness $\chi = E_1/E_2$, the coating relative thickness $\lambda = h/l$, the indenter relative radius R/l , the dimensionless average pressure p_n/E_1 , interface adhesion coefficient k , and the friction coefficient μ . An analysis of the principal shear stresses $\tau_1(x, y, z)$ is most interesting for studying the kinetics of the fatigue fracture of the surface layer. The analysis of the influence of the friction coefficient value and the contact density on the principal shear stress distribution and the amplitude values, determined by the function $\Delta\tilde{\tau}_1(z, n)$ is presented in [17] for the case of perfect interface adhesion ($k=0$). The function $\tau_1(x, y, z)$ significantly depends on the value of the parameter χ [9]. The coatings are classified as relatively hard ($\chi > 1$) and relatively soft ($\chi < 1$) depending on the relative mechanical characteristics of the surface layer. The results presented here are obtained for relatively hard coatings.

As follows from (2.15), the damage depends on the values of m and c . The amplitude values of the principal shear stresses are a function of the distance from the layer surface, that's why it is possible to neglect the factor c if the time intervals are considered respectively to N^* (the number of cycles before the first fracture). Then m becomes the only parameter, which determine the shape of the damage function.

Some results of the damage function calculations for $k=0$ and $k=100$ are presented in Fig.2. For the case where the coating is relatively thick, its thickness is almost 2 times greater than the radius of contact zone.

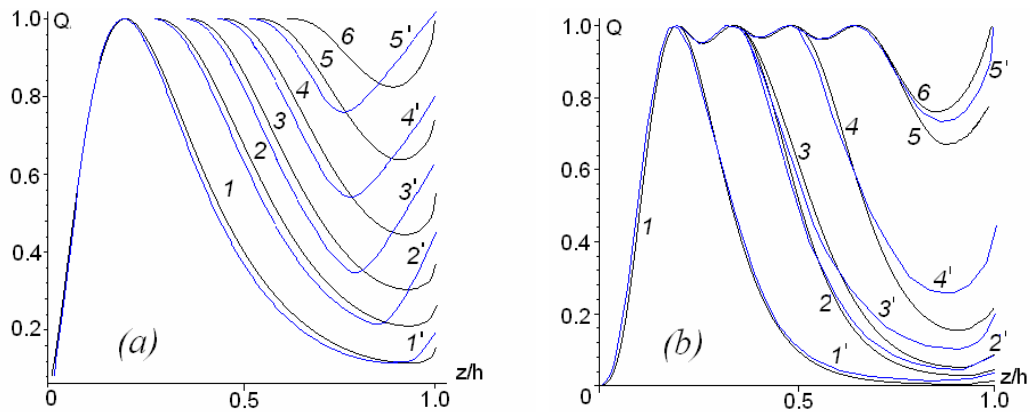


Fig.2 The damage distribution inside the elastic layer; $m = 2$ (a), $m = 5$ (b); the number of cycles: $n/N^* = 1$ (curves 1, 1'), 1.298 (curves 2, 2'), 1.611 (curves 3, 3'), 1.902 (curves 4, 4'), 2.209 (curves 5, 5'), and 2.612 (curve 6) for (a); $n/N^* = 1$ (curves 1, 1'), 2.133 (curves 2, 2'), 2.333 (curves 3, 3'), 3.599 (curves 4, 4'), 5.783 (curves 5, 5'), and 6.067 (curve 6) for (b); $k=0$ (curves 1, 2, 3, 4, 5, 6), $k=100$ (curves 1', 2', 3', 4', 5'); $\chi = 2$, $p_n/E_1 = 0.001$, $\nu_1 = \nu_2 = 0.3$, $\lambda = 0.3$, $\mu = 0.3$, $R/l = 8$.

Black curves corresponds to the case of perfect interface adhesion ($k=0$), and blue curves are constructed for the case of $k=100$. For all cases, curve 1 corresponds to the first act of the subsurface fracture. The new thickness of the layer is 0.84 of the original thickness. The further fracture process may develop in different ways. For $m = 2$, the damage function for $n > N^*$ always has two local maxima, the main maximum is at the surface and the increasing local maximum is at the layer–substrate interface. The surface wear occurs; the coating delaminating begins as the damage function comes to the critical value at the interface. For $m = 5$, the damage function after the first fracture act forms a local maximum not only at the interface but also inside the layer. This local maximum comes to the critical value, and then the next fracture occurs. For this case, there are four acts of subsurface fracture for the case of full interface adhesion ($k=0$) and three acts for the case of imperfect adhesion ($k=100$). The surface wear takes place between the fracture acts.

For both cases ($m=2$ and $m=5$) the interface imperfection leads to the increase of interface maximum of the damage function. The reason is that principal shear stress concentration at the interface is greater than that for the case of full adhesion [11].

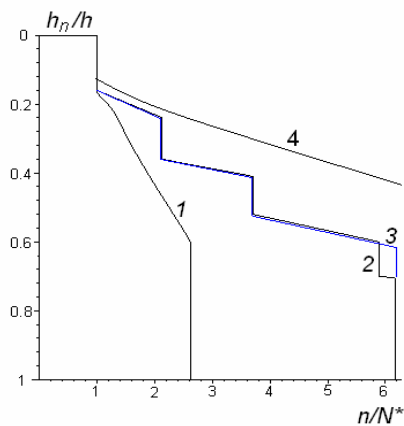


Fig.3 Evolution of the layer thickness in time; $\chi=2$ (curves 1-3), $\chi=1$ (curve 4), $p_n/E_1=0.001$, $\nu_1 = \nu_2 = 0.3$, $\lambda=0.3$, $\mu=0.3$, $R/l = 8$; $m = 2$ (curves 1, 4), $m = 5$ (curves 2, 3), $k=0$ (curves 1, 2, 4), $k=100$ (curve 3).

The results of computation of the fracture kinetics are presented at Fig. 3. Curve 4 is calculated for the homogeneous half-space with the same material elastic and strength properties ($m = 2$) as the coating material. The loading conditions coincide with the conditions for the layered half-space. The function h_n/h characterizes the displacement of the upper bound of the elastic layer (a decrease in the coating thickness) because of its fracture. The jumps correspond to the acts of subsurface fracture accompanied with detachment of the layers of coating material. Between these acts, the surface wear occurs. Note, that the interface imperfection does not influence essentially the wear rate

(see curves 2, 3). For $m = 5$, the time interval before each fracture act increases, while the thickness of the separated layers decreases. For the case of the homogeneous elastic half-space a steady-state wear process with analytically determined constant wear rate occurs [3] for frictionless sliding contact. The

computation results are obtained for the friction loading of a homogeneous elastic half-space (curve 4), and the wear rate function also tends to a constant value.

4. Conclusions

A model for calculation of the contact wear damage and simulation of the elastic layer fracture process is proposed in the study. It is obtained that for the elastic coating layer-by-layer fracture may occur as a result of damage accumulation, as well as the surface fatigue wear and the coating delaminating. The fracture process depends on the material strength properties and the amplitude values of stresses, which are determined by elastic properties of the layered half-space, the contact geometry and the layer-substrate adhesion. The wear kinetics for the layered half-space differs from the kinetics for the homogeneous half-space under the same loading conditions. The surface wear rate caused by the contact fatigue is not constant, which is accounted for by the changes of stress distributions as the surface layer thickness decreases during fracture.

Acknowledgments

The research was financially supported by the Russian Foundation for Basic Research (projects 07-01-00282a and 09-08-01236-a).

References.

1. K. L. Dahm, E. Torskaya, I. Goryacheva, and P. A. Dearnley, "Tribological Effects on Surfaces Interfaces, Proc. IMechE., Part J: J. Eng. Tribology **221** (3) (2007) 345–353.
2. Goryacheva I.G. *Contact Mechanics in Tribology*. Kluwer Academic Publishers, Dordrecht, 1998.
3. I. G. Goryacheva and O. G. Chekina, Wear of Surfaces: from Modeling of Microfracture to the Analysis of the Surface Shape Variation, Mech. Solids (Engl. Transl.) **34** (5) (1999) 104–117.
4. I. G. Goryacheva and O. G. Chekina, Model of Fatigue Fracture of Surfaces, Sov. J. Frict.Wear (Engl. Transl.) **11** (3) (1990), 389–400.
5. Makushkin A.P. Stress-strain state of elastic layer in contact with spherical indenter (I), Sov. J. Frict.Wear (Engl. Transl.), **11**(3) (1990), 423-434.
6. Makushkin A.P. Stress-strain state of elastic layer in contact with spherical indenter (II), Sov. J. Frict.Wear (Engl. Transl.), **11**(4) (1990), 602-608.
7. Kuo C.H., Keer L.M., Contact stress analysis of a layered transversely isotropic half-space, Journal of Tribology, **114**(2) (1992), 253-262.
8. Mozharovsky V.V., Rogacheva N.A., Stress state of elastic orthotropic foundation with uniform coating under the load with friction. Sov. J. Frict.Wear (Engl. Transl.), **20**(3) (1999), 289-296.
9. I. G. Goryacheva and E. V. Torskaya, A Periodical Contact Problem for a System of Dies and Elastic Layer Adhered to Another Base, Sov. J. Frict.Wear (Engl. Transl.) **16** (4) (1995) 642–652.
10. I. G. Goryacheva and E. V. Torskaya, Stress and Fracture Analysis in Periodic Contact Problem for Coated Bodies, Fatigue and Fracture of Engng. Materials and Structures **26** (4) (2003) 343–348.
11. E. V. Torskaya and I. G. Goryacheva, "The Effect of Interface Imperfection and External Loading on the Axisymmetric Contact with a Coated Solid," Wear **254** (5–6) (2003) 538–545.
12. Sainsot Ph., Leroy J.M., Villechase B., Effect of surface coatings in a rough normally loaded contact, Mechanics of Coatings (Tribology series), **17** (1990), 151-156.
13. Cole S.J., Sayles R.S., A numerical model for the contact of layered elastic bodies with real rough surfaces., Journal of Tribology, **113**(2) (1991), 334-340.
14. S. Cai and B. Bhushan, Three-Dimensional Sliding Contact Analysis of Multilayered Solids With Rough Surfaces, ASME J. Tribol., **129** (2007), 40-59.
15. E. V. Torskaya, Analysis of Friction Effect on Stress State of Coated Bodies, J. Frict.Wear (Engl. Transl.) **23** (2) (2002) 16–23.
16. V. S. Nikishin and G. S. Shapiro, *Space Problems of the Elasticity Theory for Multilayered Media*, VTs AN SSSR, Moscow, 1970 [in Russian].
17. I.G. Goryacheva, E.V. Torskaya Modeling the Contact Wear Fracture of a Two-Layer Basement, Mechanics of Solids **43** (3) (2008) 426–436.